



# Property Measurements towards Understanding Process Phenomena

Riad Abdul Abas

Licentiate Thesis

School of Industrial Engineering and Management  
Department of Material Science and Engineering  
Royal Institute of Technology  
SE-100 44 Stockholm  
Sweden

---

**Akademisk avdelning som med tillstånd av Kungliga Tekniska Högskolan i  
Stockholm, framlägges för offentlig granskning för avläggande av Teknologie  
licentiatexamen, fredagen den 3 juni 2005, kl.10:00 i B1, Brinellvägen 23, Kungliga  
Tekniska Högskolan, Stockholm**

---

*ISRN KTH/MSE--05/22--SE+THMETU/AVH*  
*ISBN 91-7178-029-7*



وہی قائم الٰہ بیت محمد (ص)



## Abstract

The main objective of this industrially important work was to gain an increasing understanding of the properties of materials such as CMSX-4 nickel base super alloy, mould powder used in continuous casting of steel and coke used in blast furnace, with special reference to the thermal diffusivities. The measurements were carried out in a wide temperature range, solid, liquid, glassy and crystalline states.

For CMSX-4 alloy, the thermal conductivities were calculated from the experimental thermal diffusivities. Both the diffusivities and conductivities were found to increase with increasing temperature. Microscopic analysis showed the presence of intermetallic phases such as NiTi and NiTi<sub>2</sub> below 1253 K. In this region, the mean free path of the phonons is likely to be limited by scattering against lattice defects. Between 1253 K and solidus temperature, these phases dissolved in the alloy adding to the impurities in the matrix, which, in turn, caused a decrease in the thermal diffusivity. This effect was confirmed by annealing the samples at 1573 K. The thermal diffusivities of the annealed samples measured at 1277, 1403 and 1531 K were found to be lower than the thermal diffusivities of non-annealed samples and the values did not show any noticeable change with time. It could be related to the attainment of equilibrium with the completion of the dissolution of  $\gamma$  and  $\gamma'$  phases during the annealing process.

Liquid CMSX-4 does not show any change of thermal diffusivity with temperature. It may be attributed to the decreasing the mean free path being shorter than characteristic distance between two neighbouring atoms.

On the other hand thermal diffusivities of mould powder having glassy and crystalline states decrease with increasing temperature at lower temperature and are constant at higher temperature except for one glassy sample.

Analogously, the thermal diffusivity measurements of mould powder did not show any significant change with temperature in liquid state. It is likely to be due to the silicate network being largely broken down.

The thermal diffusivity is increased with increasing crystallisation degree of mould powder, which is expected from theoretical considerations.

The coke sample, taken from deeper level of the blast furnace, is found to have larger thermal diffusivity. This could be correlated to the average crystallite size along the structural  $c$ -axis,  $L_c$ , which is indicative of the higher degree of graphitisation. This was also confirmed by XRD measurements of the different coke samples. The degree of graphitisation was found to increase with increasing temperature. Further, XRD measurements of coke samples taken from different levels in the shaft of the blast furnace show that the graphitisation of coke was instantaneous between room temperature and 1473 K.



## **Acknowledgment**

Special thanks to my supervisor, Professor Seshadri Seetharaman for excellent guidance and encouragement throughout the work.

I am also grateful to Dr. Miyuki Hayashi for fruitful discussions and inspiring ideas.

Thanks are also due to Professor Mamoun Muhammed, Dr. Ragnhild Aune and Dr. Anders Jakobsson for their valuable support.

Also many thanks to Dr. Robert Eriksson for his valuable help.

I thank all my colleagues working with material science in the department.

Riad Harwill Abdul Abas

Stockholm, May 2005





## Supplements

The present thesis is based on the following papers:

**Suppliment 1: Thermal Diffusivity measurement of CMSX-4 alloy by Laser flash method**  
**R. Abdul Abas, M. Hayashi and S. Seetharaman**  
**ISRN KTH/MSE--05/23--SE+THMETU/TR**  
**Submitted to International Journal of Thermophysics.**

**Supplement 2: Effect of Crystallinity on the Thermal Diffusivity of Mould Fluxes for the Continuous Casting of Steels.**  
**M. Hayashi, R. Abdul Abas and S. Seetharaman**  
**ISIJ International, Vol. 44 (2004),No. 4 (April), pp. 691-697.**

**Supplement 3: Studies on Graphitisation of Blast Furnace Coke by X-ray Diffraction Analysis and Thermal Diffusivity Measurements**  
**R. Abdul Abas, A. Jakobsson, M. Hayashi and S. Seetharaman**  
**ISRN KTH/MSE--05/24--SE+THMETU/TR**  
**Submitted to International Journal of Thermophysics.**

**My contribution to the different supplements of the thesis:**

**I.** Literature survey, experimentation and major part of the writing.

**II.** Experimentation, result evaluation, participates in the theoretical analyses.

**III.** Literature survey, participates in the theoretical analyses, experimentation and major part of the writing.



## Contents

<b>1. Introduction</b> .....	<b>1</b>
<b>1.1 Industrial importance</b> .....	<b>2</b>
<b>2. Experimental</b> .....	<b>2</b>
<b>2.1 Apparatus</b> .....	<b>3</b>
2.1.1 Laser flash equipment .....	3
2.1.2 X-ray diffractometer .....	6
<b>2.2 Material and sample arrangements</b> .....	<b>7</b>
2.2.1. CSMX-4 .....	7
2.2.2. Mould powder .....	7
2.2.3. Coke .....	8
<b>3. Results and Discussion</b> .....	<b>11</b>
<b>3.1 Thermal diffusivity measurements</b> .....	<b>11</b>
<b>3.1.1 CMSX-4 alloy</b> .....	<b>11</b>
<b>3.1.2Mould powder</b> .....	<b>14</b>
<b>3.2 XRD measurements</b> .....	<b>18</b>
3.2.1 Mould powders .....	18
3.2.2. Coke samples .....	19
<b>4. General discussion.</b> .....	<b>24</b>
<b>5. Conclusion</b> .....	<b>25</b>
<b>6. Future work.</b> .....	<b>26</b>
<b>References</b> .....	<b>27</b>



## 1. Introduction

Thermophysical properties such as thermal diffusivity, viscosity and heat capacity are very important from both fundamental as well as applied view points. There are many engineering situations in which the ability of a structural component to conduct heat to or from a material such as mould flux, high temperature resistant alloys and blast furnace coke or to dissipate a large quantity of locally generated heat is of fundamental importance. It is therefore, necessary to determine the thermal transport properties of such materials. If, however improvements in engineering efficiency are to be achieved by improving the heat transfer characteristics, it becomes necessary to understand how, for the material under investigation; heat transport is affected by changes in structure or in the relative proportion of phase's present [1].

In recent years, mathematical modelling of the heat transfer mechanism occurring in high temperature processes has resulted in improvements in process control such as steelmaking and production of heat resistance materials such as Ni-base and Ti-based super alloys. However, reliable values for the thermophysical properties of materials involved are required for the successful operation of these models [2].

To optimise the blast furnace process, the coke quality and coke consumption rate must be improved. One major factor affecting the coke quality is the degree of graphitisation. It was reported that the higher degree of graphitisation leads to lower reactivities [3,4]. Earlier studies of the thermal diffusivities of coke samples from different levels of the experimental blast furnace indicate that, as coke descends through the shaft of the furnace, the degree of graphitisation as well as thermal diffusivity increase [5,6]. It is critical to the optimum performance of the furnace to focus on the factors, which could affect the degree of graphitisation. These factors can be temperature, chemical composition, thermal history and the coke surface energy.

In the continuous casting of steels, one of the factors affecting the surface quality of the product is the heat transfer process occurring in the mould. It is dominantly influenced by the characteristics of the mould powder infiltrated into the mould/strand gap. The mould powder forms a slag film between mould and solidified steel shell, which frequently consists of glassy, crystalline and liquid layers. Because of the importance of the thermal diffusivity values of slags in heat transfer modelling, they have been measured by different researchers. With respect to the thermal conductivities/ diffusivities of mould flux powder in the glassy and crystalline state, there are very few previous reports available. Shibata et al [7] and Taylor and Mills [8] have reported that the thermal diffusivities of the crystalline samples are higher than those of the glassy samples. However, since the thermal conductivities/ diffusivities of solid slag are considered to be depending on crystallinity, the property should be measured as a function of the degree of crystallization as well as temperature. Because of the experimental difficulties in high temperature measurements, there are very few accurate data of such properties.

The aim of this study is to develop tools for monitoring the progress of a high temperature phenomenon by following the physical property and structural changes by suitable experimental techniques. The scope of the thesis covers precise measurements of

1. the thermal diffusivities of mould flux in glassy, crystalline and liquid phase,
2. effect of temperature, chemical composition, the thermal history and surface energy of the coke using thermal diffusivity and X-Ray Diffraction (XRD) measurements and

3. thermal diffusivity measurements of CMSX-4 nickel base super alloy in solid and liquid states.

The last part of the work was conducted as a part of the European Space Agency (ESA) project, THERMOLAB, for precision measurement of thermophysical properties of industrial alloys for optimisation of the industrial process design, product quality and resource composition.

## **1.1 Industrial importance**

The industrial importance of this work is to use these measurements to get a clear understanding of the phenomena underlying some industrial processes as well as to clarify the impact of structure on properties.

CMSX-4 alloy is designed as a heat resistant and creep resistant alloy for high temperature applications. At high temperatures, the material could be more ductile, but in this alloy the intermediate particles can be nucleated to be a real obstacle in front of the dislocation slip. On the other hand, these particles increase the structure disorder, which can affect the thermal conductivity.

In the continuous casting of steel, the mould powder is used to prevent the direct contact between the mould and the product. The heat transfer occurring in the mould is an important factor affecting the surface quality of the product. It is shown that the glassy and liquid states have lower conductivities than the crystalline state. Furthermore, the measurements show that the crystalline state can be controlled by chemical composition of mould powder and the process conditions such as temperature and annealing time.

The graphitisation degree of coke is affected by amorphous carbon percentage as well as temperature. The coke reactivity as well as coke consumption rate are important parameters in proper control of the blast furnace process.

## **2. Experimental**

The present work was focused on the measurements of the above-mentioned materials using two different techniques, viz. laser flash method for thermal diffusivity measurements and (XRD) analysis for structural investigations. In the following sections, brief descriptions of the techniques are provided.

## 2.1 Apparatus

### 2.1.1 Laser flash equipment

A Sinku-Rico laser flash unit (model TC-7000H/MELT), with a maximum sample temperature limit of 1873 K was used for the present thermal diffusivity measurements. A schematic diagram of the same is presented in Figure 1. The furnace heating elements, eight in number, are made of lanthanum chromate. The sample was heated in argon atmosphere at the rate of 6 K/min.

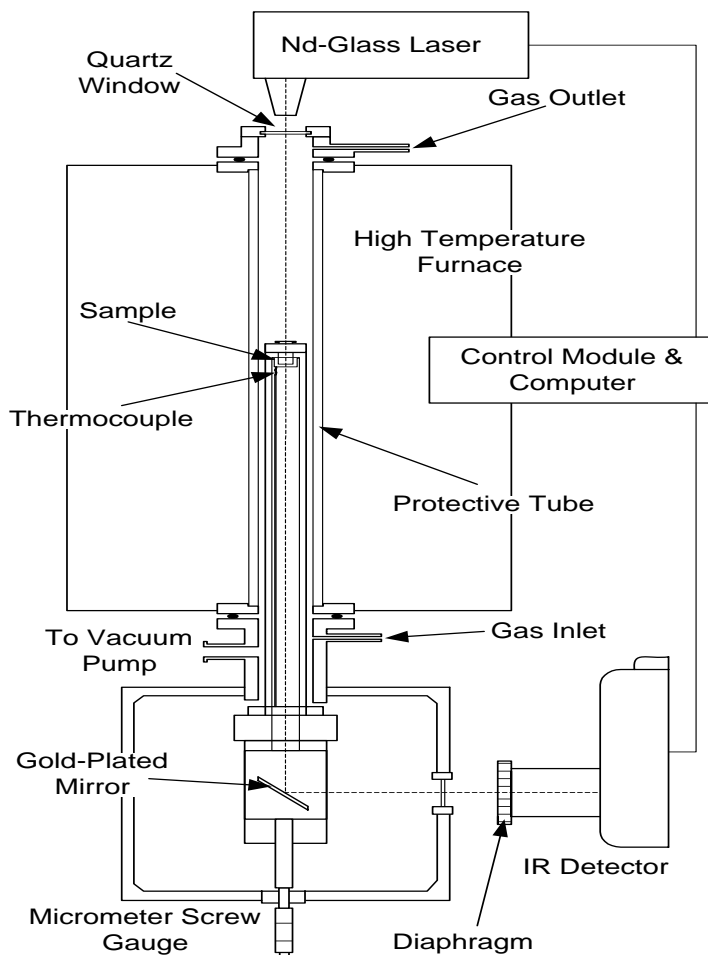


**Figure 1:** Laser-Flash unit schematic diagram

The sample temperature was measured using a Pt-13%Rh/Pt (R-type) thermocouple positioned in an alumina tube and placed closed to the sample holder. In the laser flash technique, the topside of a small disc of material is irradiated with a laser, which provides an instantaneous energy pulse. The laser energy is absorbed on the top surface of a sample and gets converted to heat energy. The thermal energy is conducted through the sample. The temperature rise at the back surface of the sample is monitored using an infrared detector. A plot of the back surface temperature against time is plotted in Figure 2. The magnitude of the temperature rise and the amount of laser energy are not required for a thermal diffusivity determination, but only the shape of the curve, which is used in the analysis. The time required for the rear surface to reach half of the maximum temperature rise is denoted as  $t_{1/2}$ . Depending on the specimen and the thermal diffusivity value,  $t_{1/2}$  can range from a few milliseconds to a few seconds. The thermal diffusivity can be expressed as:  $\alpha = 1.37L^2/\pi^2t_{1/2}$ . Where L is the sample thickness .

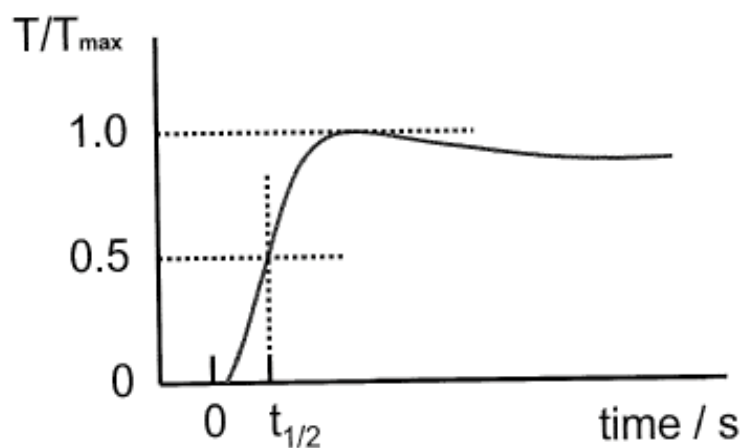


**Figure 2:** The recorded temperature history at the rear surface of a specimen calculated by instrument.

For liquid metals, the sample is sandwiched between two sapphire crucibles to get an accurate thickness as shown in Figure 3a. It is to be noted that the crucibles are transparent to the laser beam.

In the case of molten mould flux, the three-layered cell arrangement was employed. The three layers are composed of the liquid sample having the form of a thin film, sandwiched between two platinum crucibles. The laser pulse is exposed on the top surface of the upper and the temperature rise on the rear surface of the lower crucible is monitored as a function of time. The experiment is repeated by varying the sample thickness. Figure 3b shows the schematic of three-layered arrangement.



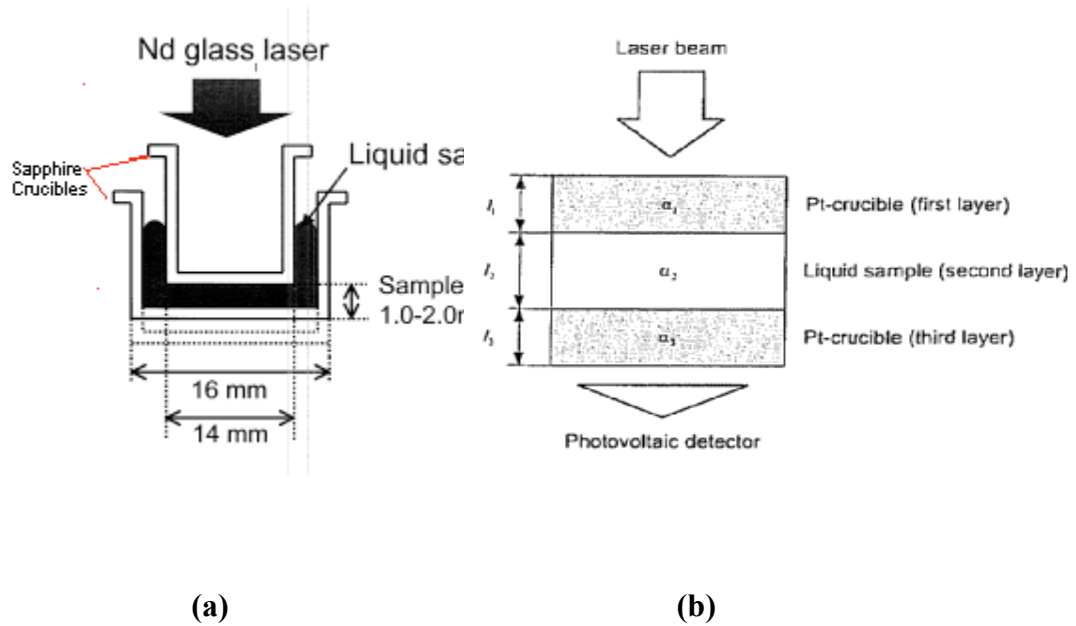


**Figure 3:** (a) Sample arrangement during liquid alloy thermal diffusivity measurement, (b) Schematic diagram shown the three-layered cell arrangement in the case of mould fluxes.

The measurements at high temperatures are carried out in an inert atmosphere in order to prevent chemical reactions with the atmosphere. The impurity levels in the commercial argon gas had to be brought down significantly, especially the oxygen potential. In order to lower the impurity levels in the argon gas, it was subjected to a number of purification steps. The gas cleaning system used in the present work is schematically presented in Figure 4. The moisture impurity in the argon gas was removed by passing the gas successively through silica gel as well as  $\text{Mg}(\text{ClO}_4)_2$ . To remove traces of  $\text{CO}_2$  in the gas, a column of ascarite was introduced in the gas-cleaning system. The gas was passed through columns of copper and magnesium turnings kept at 923 K and 723 K respectively. The final partial pressure of oxygen in the argon cleaned in this way was found by using a  $\text{ZrO}_2\text{-CaO}$  oxygen sensors to be less than  $10^{-18}$  atm.

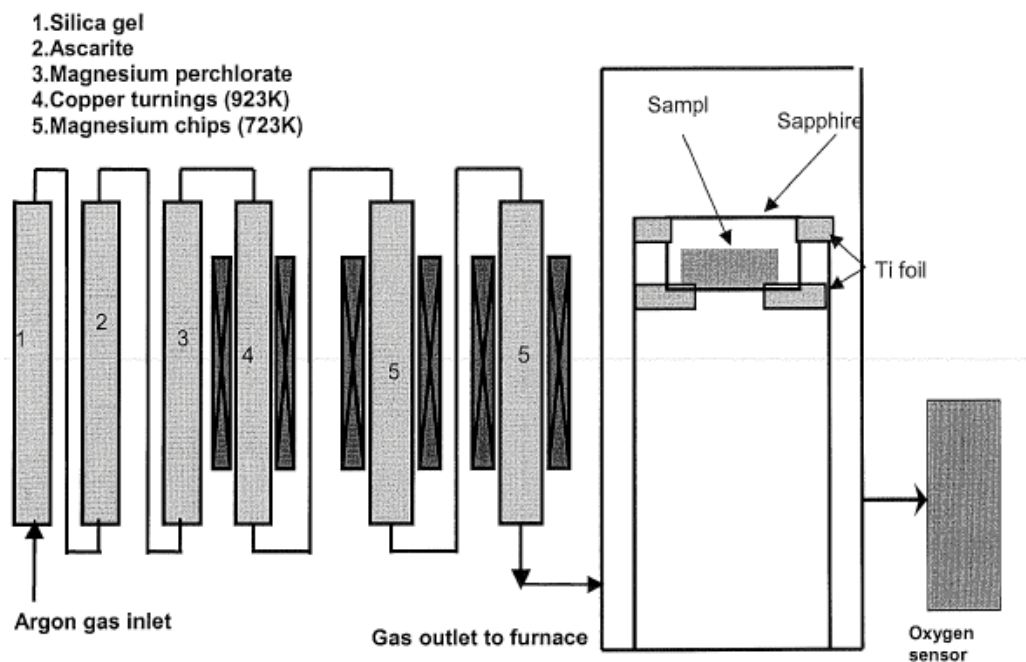


**Figure 4:** The gas cleaning system.

### 2.1.2 X-ray diffractometer

X-ray diffractometer, Philips X-pert system at the Royal Technical Institute of Technology KTH, Stockholm, Sweden was used in the present work. The samples, either milled coke or mould slag sample, was placed on the platinum strip, which could also be used as a heater. Scattering intensities from copper  $K\alpha$  (wavelength  $\lambda$  is  $1.54 \text{ \AA}$ ) were used (50 kV, 40 mA) for the diffraction studies. For coke study, it was found by preliminary trials that the peak at a  $2\theta$  value of about  $26^\circ$  was most appropriate for monitoring the graphitisation reaction. The samples were scanned over peak (002) in the scanning range  $(20-30)^\circ$  in steps of  $0.02^\circ$ . A schematic diagram of the XRD equipment is shown in Figure 5.

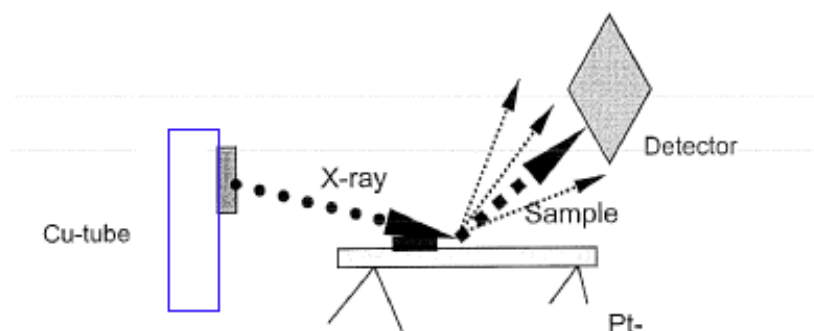


**Figure 5:** Schematic drawing of the X-ray unit

Isothermal measurements were carried out at 973, 1073, 1173, 1273, 1373 and 1473 K in order to investigate the effect of the time and temperature on the degree of graphitisation.

In the case of mould flux, X-ray diffraction studies were carried out for the glassy and crystalline samples in order to determine the phase and the degree of crystallisation. X-ray diffraction profiles of crystalline sample have shown that the component can be cuspidine ( $\text{Ca}_4\text{Si}_2\text{O}_7\text{F}_2$ ) or nepheline ( $\text{Na}_3\text{KAl}_4\text{O}_{16} \cdot \text{NaAlSi}_3\text{O}_8$ ). Because the largest peak of  $\text{Mn}_2\text{O}_3$  at  $2\theta = 32.951^\circ$  does not overlap with any crystalline peaks of the sample and the largest peak of cuspidine at  $2\theta = 29.150^\circ$  does not overlap with any of the peaks of  $\text{Mn}_2\text{O}_3$ , the degree of crystallization was defined as the ratio of the largest peak intensity of the cuspidine to that of  $\text{Mn}_2\text{O}_3$  observed for X-ray diffraction profile of the well-mixed powder of 0.1g of samples and 0.15 g of  $\text{Mn}_2\text{O}_3$ .

## 2.2 Material and sample arrangements

### 2.2.1. CSMX-4

The chemical composition of the CSMX-4 sample is given in Table I [9]. A sapphire crucible, which is transparent to laser beam and infrared rays, was used as holder. A titanium foil was placed close to sample as a local oxygen receiver in the argon gas atmosphere and, thereby to protect the sample from oxidation. Discs having 10 mm in diameter and approximately 2 mm in thickness were machined from the CSMX-4 alloy bulk to fit the experimental unit. In liquid state, the sample has been sandwiched between two sapphire crucibles in order to get accurate thickness of sample.

**Table I.** Chemical compositions in mass % (except for O and S which are in ppm) of CMSX-4 samples [9].

Al	C	Cr	Fe	Mo	O	Re	S	Si	Ta	Ti	W
5.6	0.004	6.4	0.04	0.16	2*	2.9	2*	0.4	6.5	1.05	6.4

### 2.2.2. Mould powder

The chemical compositions of the four proprietary mould powders used in Swedish steel industry are given in Table II. The mould powders were decarburised by heating in air for 48 h at 1073 K. The decarburised powders were placed in platinum crucibles and melted in air for 0.25 h at 1623 K for powder A, and at 1573 K for powders B-D. Glassy samples were prepared by pouring the melts onto a stainless steel plate kept at 773 K. Subsequently, the samples were annealed in air for 1h at 773 K and cooled down by the furnace-cooling rate to eliminate the residual stress. Discs having about 12 mm in diameter and 1.5 to 2.5 mm in thickness were machined from the glassy samples. Annealing of the glassy samples having the disc shape at 1073 and 1173 K for 1-120 h led to their crystalline structure. Since the surfaces of the annealed samples became very rough because of the crystallization, the surfaces were polished to obtain the parallelism between both faces.

**Table II.** Chemical compositions of the proprietary mould powders (mass%).

	A	B	C	D
SiO <sub>2</sub>	25.5	32.7	34.2	28.8
CaO	22.7	28.8	29.4	36.5
MgO	0.97	1.77	1.01	1.3
Al <sub>2</sub> O <sub>3</sub>	12	4.7	3.92	6.5
TiO <sub>2</sub>	0.46	0.11	0.1	0.3
Fe <sub>2</sub> O <sub>3</sub>	2.86	1.24	1.09	0.8
MnO	0.04	< 0.10	0.05	3.3
Na <sub>2</sub> O	2.62	11.3	12.8	7.2
K <sub>2</sub> O	1.43	0.31	0.37	0.1
F	4.42	9.4	7.95	5.9

### 2.2.3. Coke

The sampling scheme of coke taken out from the Experimental Blast Furnace EBF at MEFOS Luleå, Sweden is schematically depicted in Figure 6. Coke sampling was carried out after nitrogen quenching followed by a carefully documented dissection, where approximately 20-35 pieces were taken out at different radial locations and different levels. The samples (approximately 6-8 cm<sup>3</sup>) used in the present investigation are denoted as KL05, KL25, and KL35. The distance (mm) of the levels KL05, KL25 and KL35 from the top are about 3961, 6652 and 6981 mm respectively. At each level, coke samples were taken from the centre (C), the place just beside the wall (R) and in between (M).

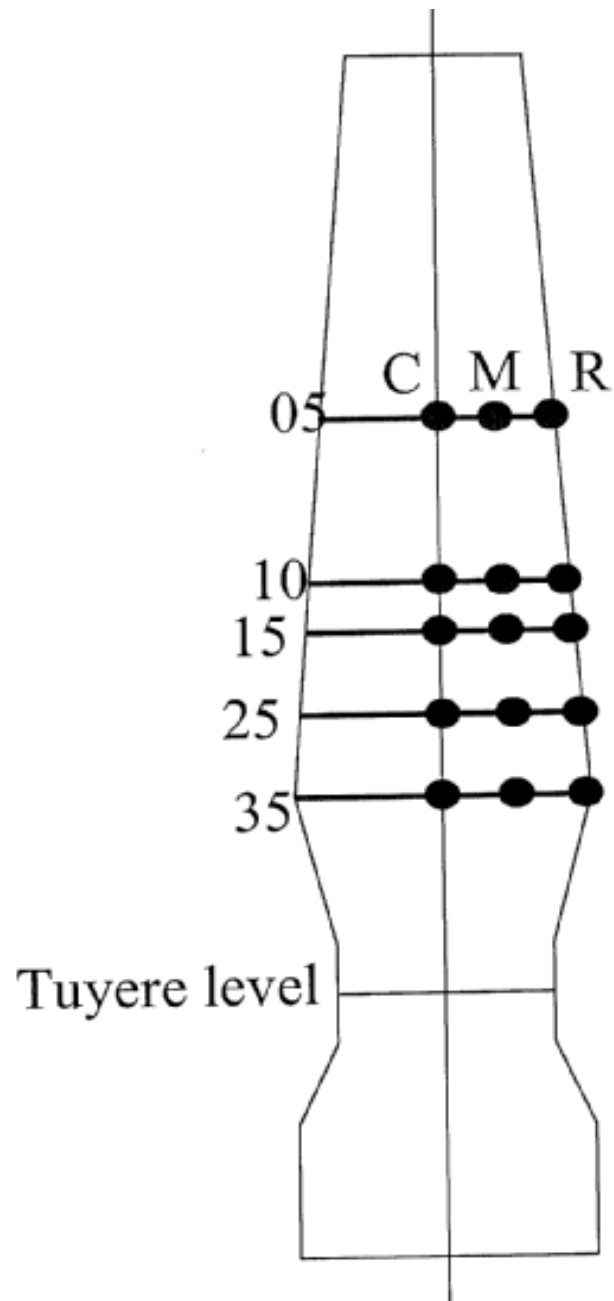


**Figure 6:** Schematic diagram of the experimental blast furnace [3].

A chemical analysis of the samples from the quenched pilot blast furnace is presented in Table III. Pellets having 10 mm in diameter and approximately 3 mm in thickness were machined from coke lumps to fit the experimental unit specification.

**Table III.** Chemical analysis in wt% of coke samples from the experimental blast furnace [3].

	Fe [%]	CaO [%]	SiO <sub>2</sub> [%]	P <sub>2</sub> O <sub>5</sub> [%]	S [%]	Al <sub>2</sub> O <sub>3</sub> [%]	MgO [%]	Na <sub>2</sub> O [%]	K <sub>2</sub> O [%]	TiO <sub>2</sub> [%]	C [%]
<b>Feed</b>	0.4	0.08	6.12	0.03	0.58	2.85	0.06	0.13	0.15	0.17	89.43
<b>05C</b>	0.42	0.01	5.76	0.03	0.59	2.63	0.06	0.1	0.17	0.16	90.17
<b>10C</b>	0.46	0.04	6.39	0.03	0.5	2.77	0.06	0.16	0.35	0.17	89.11
<b>15C</b>	0.37	0	6.3	0.024	0.54	2.65	0.06	0.43	1.24	0.15	88.34
<b>20C</b>	0.32	0.02	5.58	0.023	0.51	2.57	0.07	0.61	1.78	0.14	88.48
<b>25C</b>	0.32	0.02	5.83	0.024	0.47	2.61	0.08	0.67	2.31	0.14	87.61
<b>30C</b>	0.34	0.04	5.97	0.025	0.5	2.66	0.08	0.68	2.07	0.14	87.61
<b>35C</b>	0.27	0	5.81	0.22	0.44	2.64	0.08	0.85	3.21	0.12	86.66
<b>05M</b>	0.49	0.07	6.22	0.029	0.54	2.85	0.08	0.14	0.2	0.18	89.25
<b>10M</b>	0.45	0.06	6.17	0.031	0.56	2.7	0.07	0.2	0.35	0.17	89.32
<b>15M</b>	0.4	0.05	6.15	0.031	0.51	2.8	0.22	0.48	1.67	0.14	87.63
<b>20M</b>	0.29	0.03	5.93	0.022	0.47	2.65	0.09	0.83	2.71	0.13	86.94
<b>25M</b>	0.31	0.03	5.41	0.022	0.49	2.43	0.09	0.75	2.43	0.13	88.02
<b>30M</b>	0.33	0.01	5.86	0.022	0.48	2.65	0.07	0.91	2.92	0.12	86.7
<b>35M</b>	0.27	0.04	5.78	0.019	0.43	2.61	0.12	1.22	3.54	0.11	85.95
<b>05R</b>	0.4	0.05	6.34	0.029	0.54	2.95	0.07	0.13	0.25	0.17	89.17
<b>10R</b>	0.96	0	10.64	0.012	0.16	1.73	9.19	0.82	1.91	0.05	74.18
<b>15R</b>	0.25	0.03	5.63	0.023	0.44	2.54	0.1	1.05	3.65	0.11	86.28
<b>20R</b>	0.24	0.03	5.58	0.03	0.54	2.68	0.11	1.17	3.96	0.11	85.71
<b>25R</b>	0.23	0.04	5.95	0.022	0.4	2.61	0.14	1.32	4.7	0.1	84.58
<b>30R</b>	0.22	0	5.65	0.023	0.43	2.54	0.1	0.93	5	0.09	85.13
<b>35R</b>	0.22	0	5.53	0.02	0.42	2.41	0.09	1	4.49	0.1	85.83

### 3. Results and Discussion

The measurements of thermal diffusivity of CMSX-4 nickel base super alloy as a function of temperature was undertaken. The influence of crystallisation degree and temperature on the measured thermal diffusivity of four types of mould powder was also carried out.

XRD measurements were carried out to investigate the effect of time, temperature and chemical composition on the graphitisation phenomenon of coke using in the blast furnace. Furthermore, XRD analysis was employed in order to determine the crystallisation degree as a function of annealing temperature and time and effect of crystallisation degree on the thermal diffusivity of mould powder.

#### 3.1 Thermal diffusivity measurements

##### 3.1.1 CMSX-4 alloy

During thermal diffusivity measurements, the CMSX-4 samples were heated to 1573 K and cooled to room temperature at a rate of 6K/min. In order to get an accurate data, three (heating-cooling) cycles and one heating cycle were carried out. Figure 7 shows that the thermal diffusivity is increased with temperature up to about 1223 K. The thermal conductivity,  $\kappa$ , can be considered to be due to lattice vibrations, *viz.* phonon conduction. According to Debye [10], the thermal conductivity can be expressed by the equation:

$$\kappa = \frac{1}{3} n C_v v l \quad (1)$$

where  $n$  is the number of particles per unit volume,  $C_v$  is the heat capacity at constant volume per particle (so that  $n.C_v$  is the heat capacity per unit volume expressed in  $J/km^3$ ),  $v$  the velocity of sound and  $l$  is the phonon mean free path. Assuming that the velocity of sound,  $v$ , is constant, the thermal conductivity will be proportional to the phonon mean free path. The term  $l$  is dependent on collision between phonons as well as with lattice defects. In the present case, the thermal conductivity,  $\kappa$ , was found to increase with temperature and can be considered as proportional to  $T^n$ . At lower temperatures, collisions between phonons are less significant compared to the phonon scattering against defects. If  $l$  is independent of  $T$ , the thermal conductivity will be proportional to  $C_v$ , which, in turn, is approximately proportional to  $T^3$  [11]. The situation in the present case is complicated due to the industrial sample being investigated, where the precipitation of intermediate phases like NiTi and NiTi<sub>2</sub> ( $\gamma$  and  $\gamma'$  phases) might not have reached equilibrium state. After fast quenching from this range of temperatures, the samples were analysed using SEM. By using the TEM, the chemical composition of the particles, grains and matrix were analysed. As shown in Table IV the

intermediate particles were NiTi and NiTi<sub>2</sub>. These intermediate components have been marked in Figure 8.

At later stages, the thermal conductivity shows constancy or a slight decrease with temperature. This could be that, in this range of temperatures, the intermediate phases, which have nucleated, start to dissolve in the matrix. The variation of thermal diffusivity with temperature can be attributed to a) thermal diffusivity of the  $\gamma$  and  $\gamma'$  phase particles remaining is lower than that of the matrix and grain [12]; b) as the impurity level in the matrix increases due to the dissolution of  $\gamma$  and  $\gamma'$  phases, the disorder of the alloy increases, which decreases the mean free path of the phonons, c) part of the heat energy supplied by the laser shot is absorbed at phase transformation *viz.* the dissolution of  $\gamma$  and  $\gamma'$  phases. Figure 9 (and even Figure 7) shows that there is no significant change in the thermal diffusivity values after annealing during isothermal measurements at 1277, 1403 and 1531 K as a function of time or temperature and that the values obtained after annealing are lower than those measured without annealing treatment. This is indicative of the attainment of thermodynamic equilibrium, where the dissolution of the intermediate phases in the matrix might have been complete and the attainment of impurity levels in the matrix was in maximum.

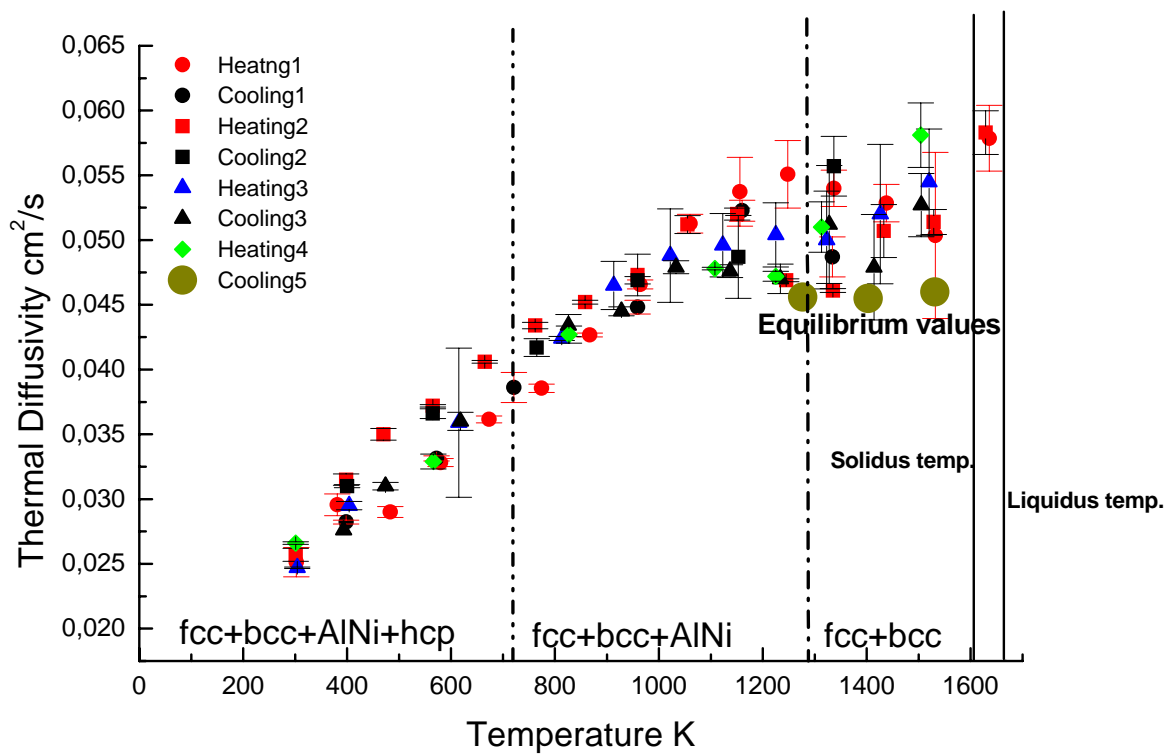
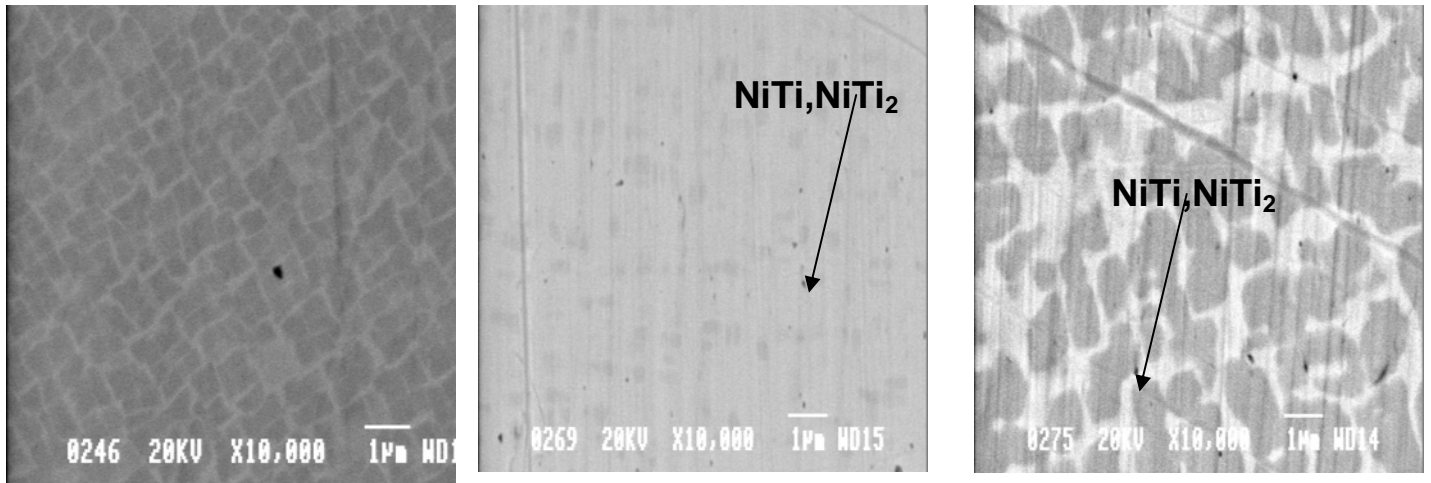


**Figure 7:** Thermal diffusivity-temperature curves of CMSX-4 alloy including the equilibrium values.





a

b

c

**Figure 8:** SEM pictures of CMSX-4 alloy during: (a) not heat-treated. (b) quenched from 1373 K after 30 min waiting time. (c) quenched from 1373 K after heating to 1573 K and keeping 12 hr and cooling to 1373 K.

**Table IV.** Chemical analysis of CMSX-4 alloy phases using TEM after heat-treating at 1573 K and cooling to 1373 K shown in Figure 8c.

Spectrum	O	Al	Si	Ti	Cr	Co	Ni	Mo	Ta	W	Total	Remarks
Particle( $\gamma$ )	14.93	2.30	0.33	30.51	2.48	5.82	40.76	0.19		2.69	100.00	<i>NiTi, NiTi<sub>2</sub></i>
Grain		4.13	0.17	0.93	2.53	9.31	76.09	0.01	2.68	4.16	100.00	
Matrix		1.27	0.99	0.41	11.86	17.02	64.64	0.04	0.07	3.30	100.00	

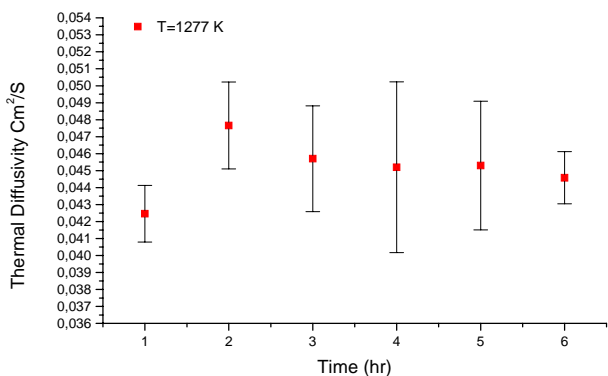
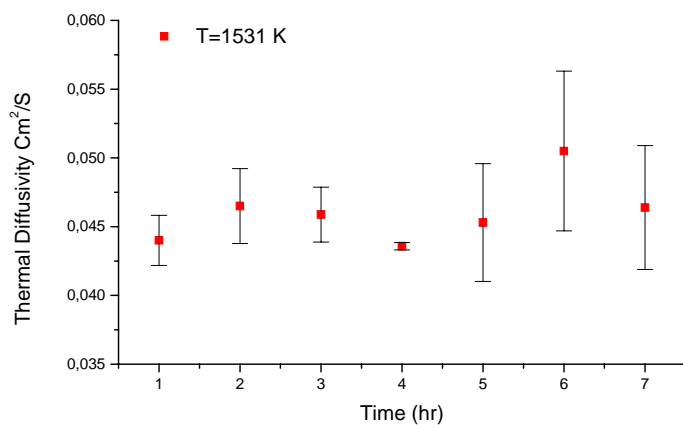
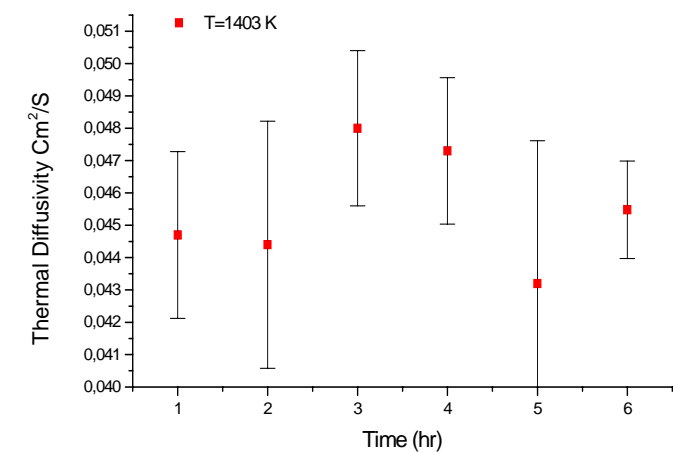


**Figure 9:** Thermal diffusivity-time curves at 1277, 1403 and 1531 K.

### 3.1.2 Mould powder

In the case of the mould flux measurements, Figure10 shows the temperature dependences of the thermal diffusivities of the glassy samples and the samples annealed at 1073 K for 1-120 h for powder A, 1-15 h for powder B and 1 h for powder C and D respectively. Closed symbols are data recorded during the heating cycles and open symbols during the cooling cycles.

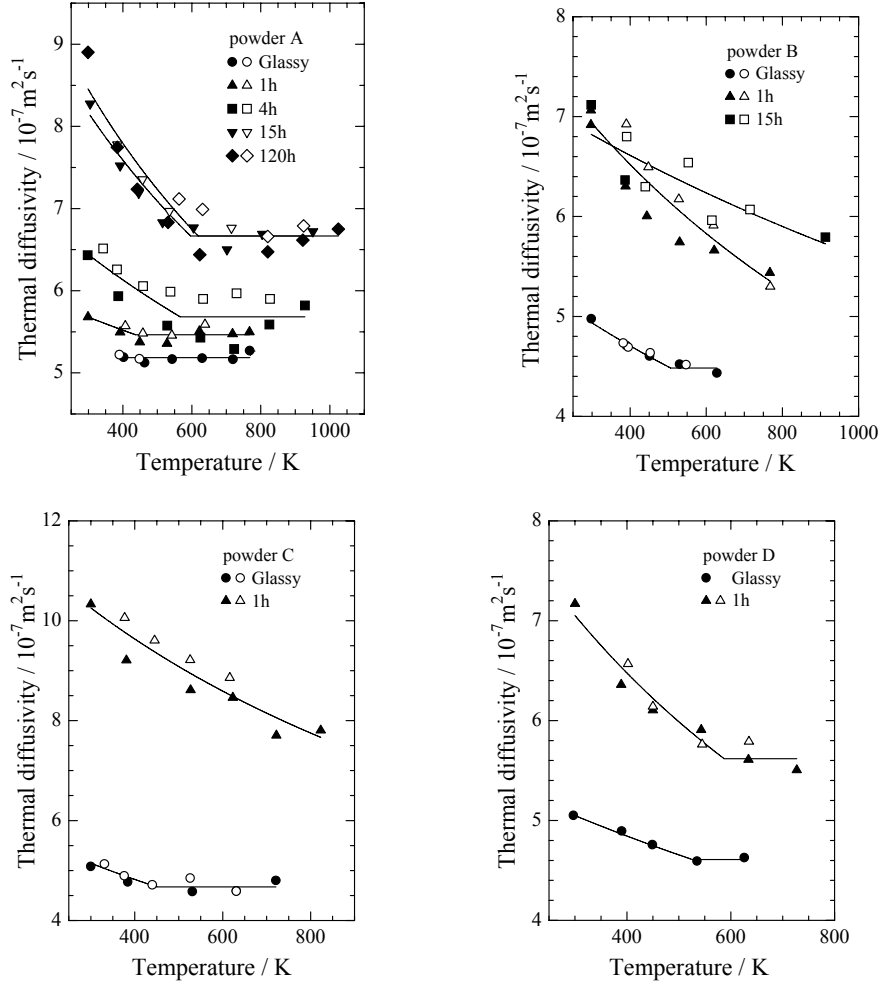


**Figure 10:** Temperature dependencies of the thermal diffusivities of the glassy and crystalline samples for powders B, C and D, respectively.

It can be seen from these figures that the thermal diffusivities of the crystalline samples decrease with increasing temperature at lower temperatures and are roughly constant at higher temperatures. These temperature dependencies were in agreement with those reported by Shibata et al [13]. It can be also seen that the sample annealed for longer time exhibits larger thermal diffusivity in the case of powder A.

Thermal conductivity is determined by lattice vibration (phonon conduction) in insulators. From the definition of the thermal diffusivity  $\alpha$ ,

$$\kappa = \alpha \rho C_p \quad (2)$$

where  $\rho$  and  $C_p$  are the density and the heat capacity respectively. Since  $C_v \approx \rho C_p$ , Eqs. (1) and (2) yield,

$$\alpha = \frac{1}{3} v l \quad (3)$$

If it is assumed that the value of  $v$  is constant irrespective of temperature, the thermal diffusivity is proportional to the phonon mean free path. As mentioned earlier, the phonon

mean free path is determined principally by two mechanisms, geometrical scattering, i.e., the collisions of phonons with the crystal boundary, lattice imperfections and so on, and phonon-phonon interaction, i.e., so-called umklapp process. The reciprocal of the effective mean free path  $1/l$  is found by adding the reciprocal of the mean free path for geometrical scattering  $l_{geo}$  and that for phonon-phonon interaction  $l_{p-p}$ , as follows;

$$\frac{1}{l} = \frac{1}{l_{geo}} + \frac{1}{l_{p-p}} \quad (4)$$

Generally, above room temperatures, the geometrical scattering is independent of temperature. On the other hand, the mean free path, determined by phonon-phonon interaction is inversely proportional to temperature above the Debye temperature[10]. Therefore, Eq. (4) is rewritten as

$$\frac{1}{l} = a + bT \quad (5)$$

where  $T$  is the absolute temperature and  $a$  and  $b$  constants. If the temperature is raised to a sufficiently high level, the mean free path decreases to a value near the lattice spacing, and is expected to be independent of temperature [14]. The solid lines in the figures have been drawn based on Eq. (5). Figure 11 shows the temperature dependencies of the thermal diffusivities of the glassy sample and the samples annealed for 1 h at 1073 and 1173 K for powder A.

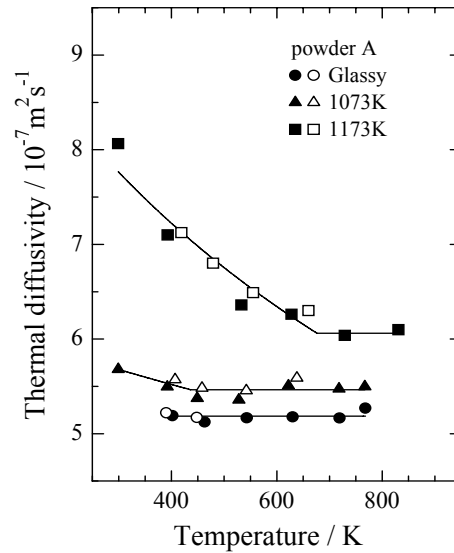


**Figure 11:** Temperature dependencies of the thermal diffusivities of the glassy sample and the samples annealed for 1 h at 1073 and 1173 K for powder A. Closed symbol are data recorded during the heating cycles and open symbols during the cooling cycles.

It can be seen from Figure 10 that, while the thermal diffusivity of the glassy sample of powder A is constant irrespective of temperature, the thermal diffusivities of the glassy

samples of powders B-D decrease with an increase in temperature at lower temperatures and are constant at higher temperatures. It is also found that the constant value of the thermal diffusivity for powders B-D is lower than that of powder A. Thermal diffusivity of a glassy sample becomes constant independent of temperature when the mean free path is limited to a fixed value by the random network structure. The randomness of the network can be estimated by the ratio of non-bridging oxygen (NBO) atoms / (Si+Al atoms), the ratio being denoted by  $NBO/\tau$  [15]. The  $NBO/\tau$  ratios of powders A, B, C and D can be calculated to be 0.92, 1.48, 1.65 and 2.11, respectively, in the manner proposed by Mills [16] by assuming that fluorine predominantly bonds to calcium rather than other cations [17] and that  $CaF_2$  does not contribute to the breakage of the silicate network [18]. Consequently, the glassy sample of powder A has less random network structure, resulting that the mean free path limited by the network structure is larger than those of other powders. On the other hand, the thermal diffusivities of the glassy samples for powders B-D show roughly the same values of  $4.6 \times 10^{-7} m^2 s^{-1}$  despite of the different  $NBO/\tau$  ratios. As shown in Figure 11, the apparent thermal diffusivities of the liquid samples for powders B-D also show similar values, *viz.*  $4.0 \times 10^{-7} m^2 s^{-1}$ . It is considered that, because the silicate network is largely broken down, there is not a significant change of structure among powders B-D. This tendency has been also shown in the previous data [19].

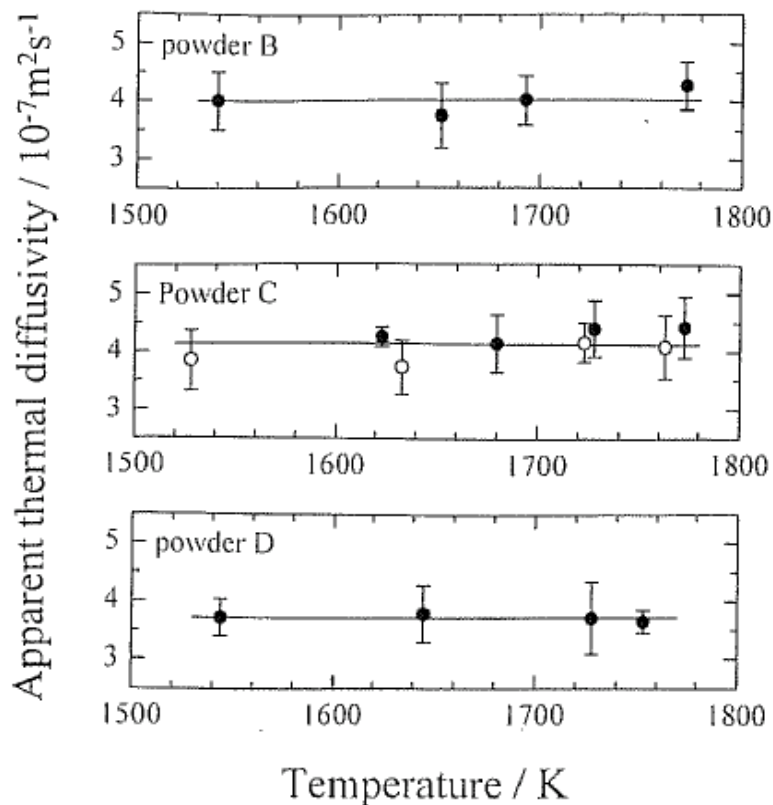


**Figure 11:** Temperature dependencies of the apparent thermal diffusivities of liquid samples of powders B-D.

## 3.2 XRD measurements

### 3.2.1 Mould powders

X-ray diffraction profiles of all glassy samples indicate no traces of crystalline phases, indicating that all glassy samples are amorphous from the viewpoint of x-ray diffraction. Figure 12 shows the x-ray diffraction profiles of the glassy sample (a) and the samples annealed at 1073 K for 1 h (b) and 15 h(c) for powder A. It can be seen that Figure 12(a) corresponds to the glassy structure. On the other hand, in Figure 12(b), which corresponds to that for the sample annealed at 1073 K for 1 h, two sharp peaks appear together with the hallow pattern due to the amorphous phase. Two sharp peaks may be attributed to nepheline ( $\text{Na}_3\text{KAl}_4\text{Si}_4\text{O}_{16}$ ,  $\text{NaAlSiO}_4$ ). On the other hand, Figure 12(c) shows that the hallow pattern disappears and only sharp peaks are observed for the sample annealed at 1073 K for 15 h, indicating that the sample has been mostly crystallized. Markings have been made at the angles where the diffraction peaks attributed to cuspidine ( $\text{Ca}_4\text{Si}_2\text{O}_7\text{F}_2$ ) and nepheline ( $\text{Na}_3\text{KAl}_4\text{Si}_4\text{O}_{16}$ ,  $\text{NaAlSiO}_4$ ) should be observed.

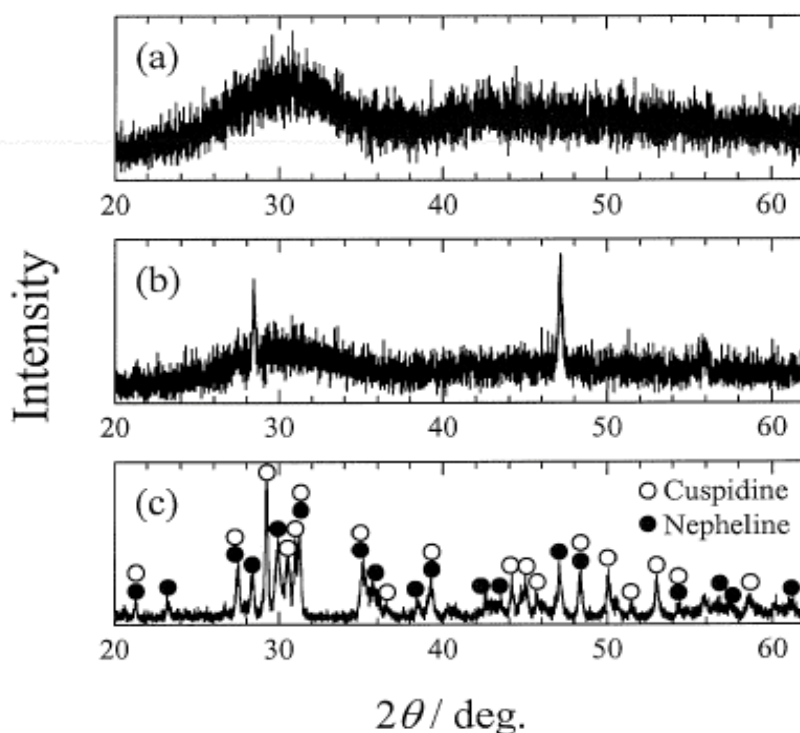


**Figure 12:** X-ray diffraction profiles of the glassy sample(a) and the samples annealed at 1073 K for 1 h(b) and 15 h(c) for powder A.

Figure 13 shows the X-ray diffraction profiles of the samples annealed at 1073 K for 1h for powders B-D. Marking has been made at the angles where the diffraction peaks attributed to cuspidine and nepheline should be observed for powder B, and at the angles where the peaks due to cuspidine should be observed for powders C and D.

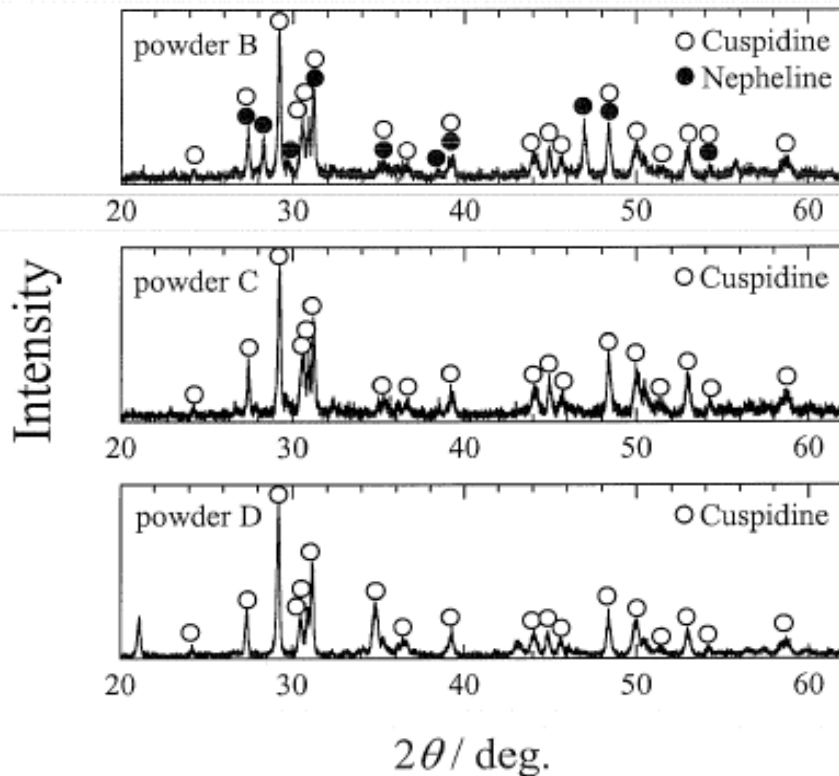


**Figure13:** X-ray diffraction profiles of the samples annealed at 1073 K for 1 hfor powder B-D.

### 3.2.2. Coke samples

The XRD isothermal measurements of blast furnace coke were carried out at 973, 1073, 1173, 1273, 1373 and 1473 K in order to investigate the effect of time on the degree of graphitisation at these temperatures. Figure 14 shows the isothermal x-ray diffractograms of coke KL35R at 1273 K. It can be seen that there is no evident change of peaks width as well as intensities i.e. the degree of graphitisation does not change with time. This could be due to the high surface energy of the coke, which gives a sudden phase transformation at high temperature. Similar behaviours were noted in the case of coke KL25C and KL05R in temperature range between 973 and 1473 K. The figure shows also there is a slight shift of the position of 002 peaks from room temperature and 1273 K. It could be attributed to the thermal expansion of the lattice parameter ( $d$ ) with increasing temperature.

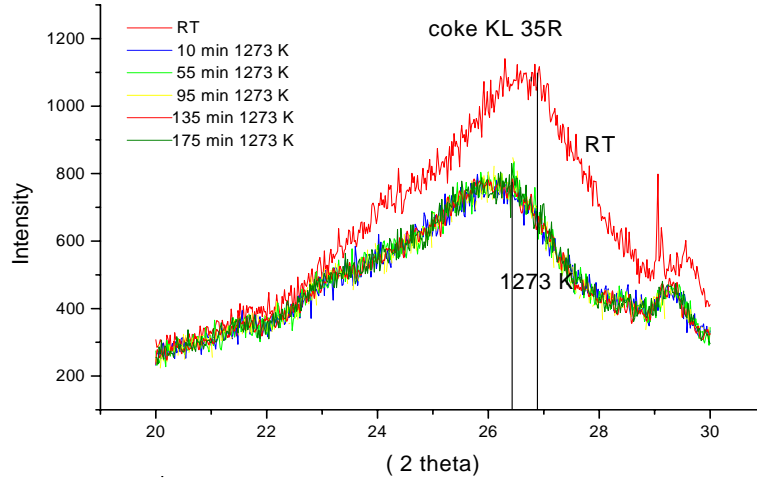


**Figure 14:** X-ray diffractograms of peak (002) during isothermal measurements at 1273 K of coke KL35R.

Figure 15 shows the XRD diffractograms during non-isothermal measurements of same coke samples. The decreasing of maximum intensities of the peaks with increasing temperature could be due to increase the atom and molecules vibration about their equilibrium position, which makes the diffraction intensities weaker [20].

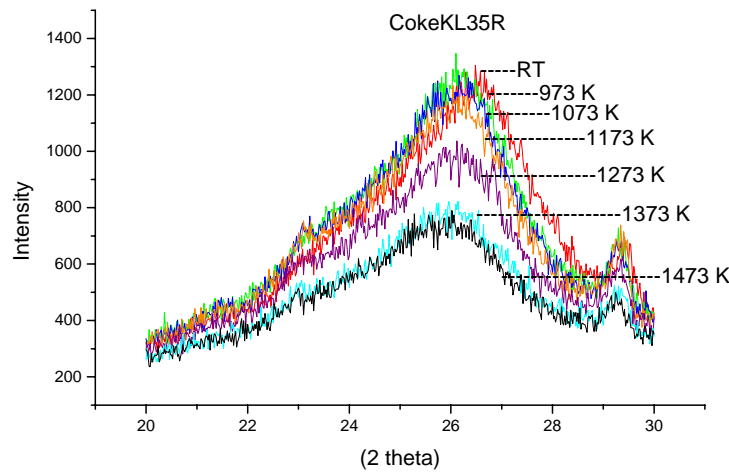


**Figure 15:** XRD diffractograms during non-isothermal measurements of coke KL35R.

The vertical dimension of carbon crystallite  $L_c$  was calculated from XRD data using Scherrer formula:

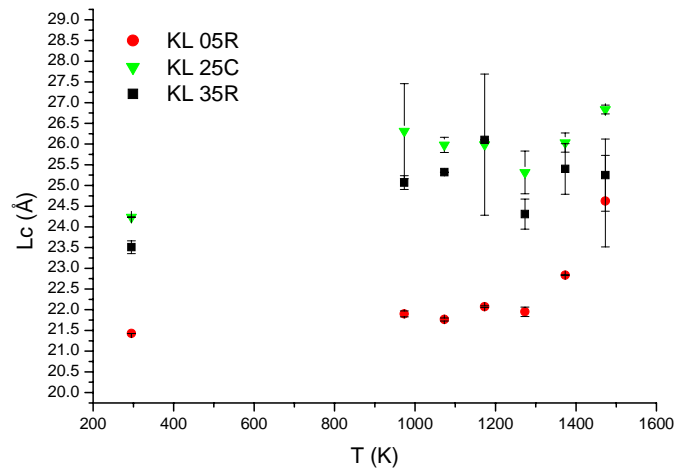
$$L_c = K \lambda / B \cos \theta \quad (6)$$

Where,  $K$  is the shape factor =0.9,  $B$  is the width of the width of the peak (002) at half intensity (radian) and  $\theta$  is position of the (002) peak.

Figure 16 shows the calculated  $L_c$  of non-isothermal XRD diffractograms versus temperature. The figure includes error bar, which are estimated from the calculation of ( $L_c$ ) by using eq.

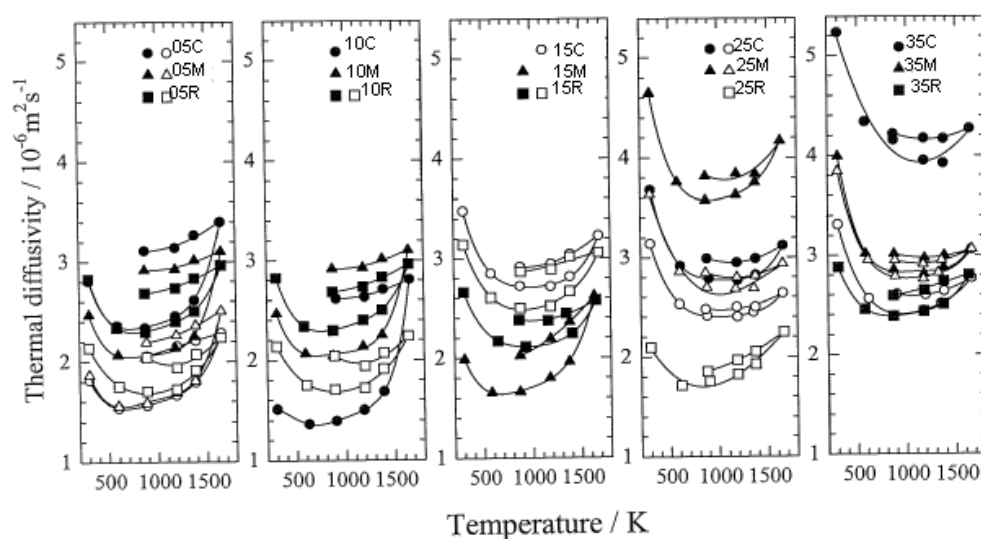


(6). Both the width of the peak as well as the intensity are difficult to establish with high accuracy from XRD plots, especially for amorphous peaks, when there is a higher degree of graphitisation and a lower amount of amorphous carbon in the KL25C and KL35R at high temperature. The figure also shows that ( $L_c$ ) is lower in coke 05R than in coke KL25 and KL35. This may be due to a higher amorphous carbon percentage of coke 05R, which was taken from the top level of blast furnace at 1073 K compared to coke 25C and 35R, which were taken from the lower level at 1623 K, where the amorphous carbon content is lower.  $L_c$  results reported here are in good agreement with those of the same coke samples at room temperature [3,4].



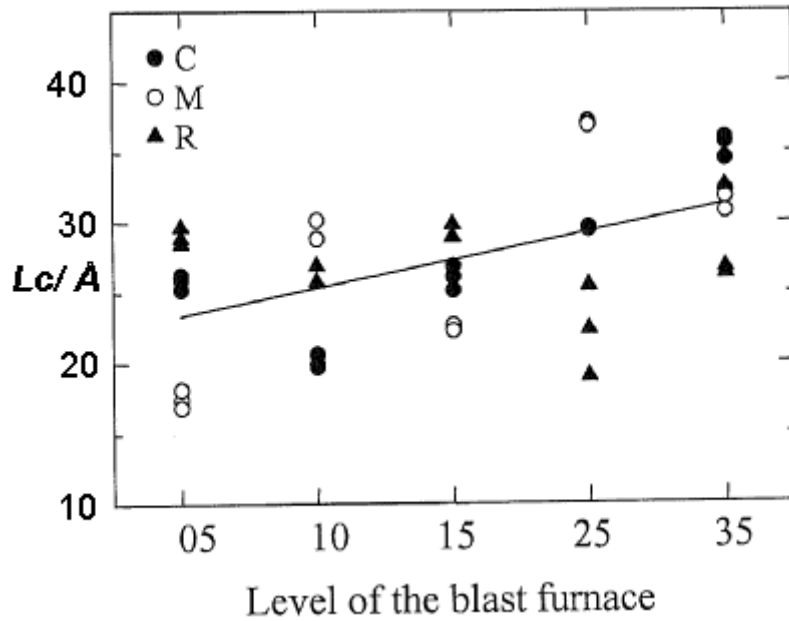
**Figure 16:** Dependence of degree of graphitisation on temperature of EBF coke.

It can be seen from Figure 17 that the coke samples taken from deeper level of the blast furnace show larger thermal diffusivities. This level dependency of the thermal diffusivity is discussed in terms of the porosity, the degree of graphitization and ash content.



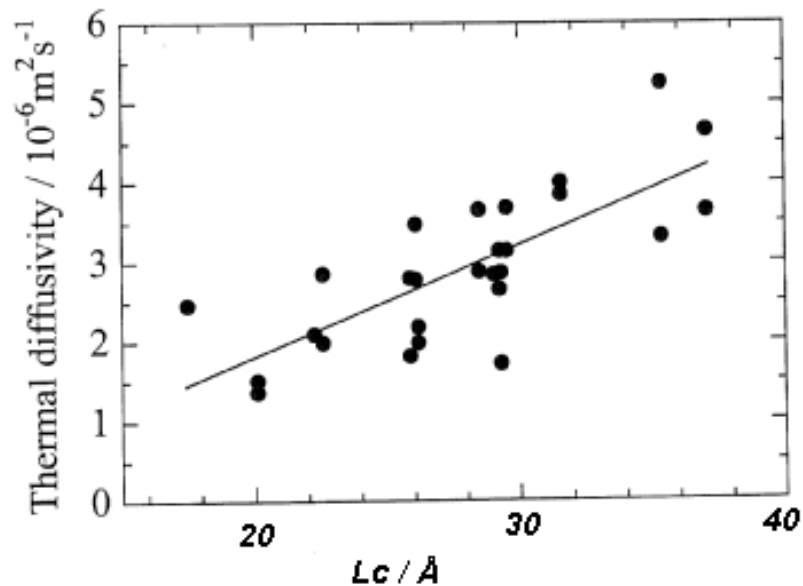
**Figure 17:** Temperature dependence of the apparent thermal diffusivities for coke samples taken from the levels 05-35.

Figure 18 shows that the coke samples taken from deeper level of the blast furnace show larger graphitisation degree. It can be due to the thermal history of the coke samples.



**Figure 18:** Values of  $L_c$  versus level of the blast furnace.

Figure 19 shows that the thermal diffusivity increases with increasing the value of  $L_c$ , i.e. the degree of graphitization. This result may indicate that the thermal diffusivity of coke sample depends on the degree of graphitization.



**Figure 19:** Thermal diffusivity at room temperature versus the average crystallite size along the structural c-axis,  $L_c$ .

Temperature dependence of (Lc) was calculated using the Arrhenius type of equation:

$$Lc = A \exp(-Q/RT) \quad (7)$$

where A is the exponential constant, R is the gas constant and Q is an energy term. The values of Q with respect to the non-isothermal graphitisation of coke KL05R, KL25C and KL35R were 2.793, 0.8904 and 1.516 kJ/mol respectively.

The energies associated with the temperature dependence of Lc are quite low in comparison with the activation energies of graphitisation using TG or DTA of different carbonious materials, which was about 120-250 kJ/mol. However, as noted earlier the instantaneous transformation is caused by the first stage of transformation, which consist the elimination of single interstitial atoms, while the reported data may include the energies of C-C breaking stage and formation and transformation of atoms and vacancies stage. Fitzer et al [21] have reported that the second stage required about 273 kJ/mol.

Figure 20 shows that d-spacing increase from room temperature to 973 K for all samples. This is likely to be due to the thermal expansion of the lattice. At temperatures above 973 K graphitisation occurs, which decreases d-spacing. At the same time, there is thermal expansion due to temperature increase. It is seen in the Figure 20 that, despite the scatter, final change in d-spacing will be small.

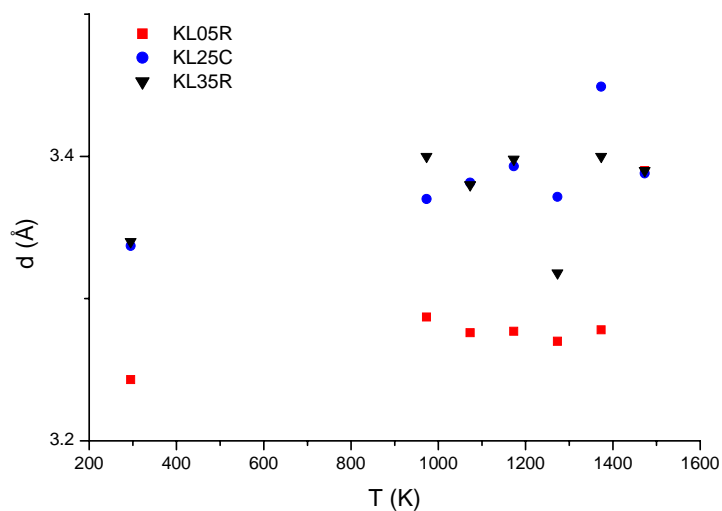


**Figure 20:** The effect of the temperature on inter- layer spacing (d).

#### 4. General discussion

The thermal transport by phonons refers to the lattice thermal conductivity, which is denoted as  $\kappa_{ph}$ . The lattice thermal conductivity is infinite if the phonon mean free path  $l$  is not limited by collision between phonons themselves or between phonons and lattice defects. Energy and momentum are conserved in a collision event, but because the phonons are massless particles, they may be annihilated or created. As mentioned in equation (4), the phonon mean free path  $l$  is limited by collision with other phonons and with lattice defects [11]. At high temperatures, the thermal conductivity must involve three or more phonons. It could be divided into two phenomena; a) when two phonons combine in a ‘collision’ event, and form one new phonon as shown in Figure 21, a. In this case ‘ $n$ ’ in equation (1) with proportion to  $T$  as it shown in linear part in Figure 7 of CMSX-4 alloy; b) when one phonon is annihilated to form two new phonons, Figure 21,b. In this case  $l$  is lead to  $1/T$  as denoted in Figure 10 and 17 of the mould powder and coke respectively.

There may also be four phonons process as shown figure 21 c and 21 d. In this case  $l$  can be proportional to  $T^2$  or  $1/T^2$  respectively. At high temperature the disordering is increased, which decreases the mean free path as well as thermal diffusivity as shown in the second part of Figure 7.

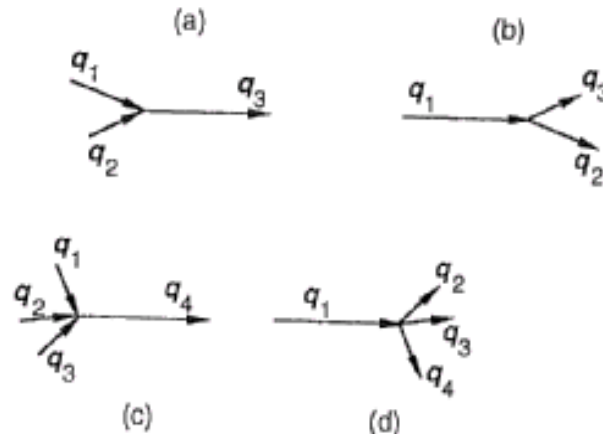


**Figure 21:** Three phonon (a,b) and four-phonon (c,d) scattering processes [11].

Analogously, the thermal diffusivity is increased with increasing the structure ordering i.e. crystallization degree by increase annealing time as well as annealing temperature of mould flux Figure (10,11). This increase could be due to reducing of point defects and crystal boundaries.

In liquid state, the disordering will be very high because of collision increasing between phonons themselves and phonon-electron. In this case the mean free path will be shorter than a characteristics distance between two neighbouring atoms. At that time the thermal

diffusivity will be independence on temperature as shown in liquid CMSX-4 and liquid mould flux Figure 9,11 respectively.

On the other hand the crystallization degree is dependant on the chemical composition of material and the heat treatment condition (time, temperature) as shown in coke and mould flux materials.

## 5. Conclusion

Properties measurements have been carried out of some industrial materials such as CMSX-4 nickel base super alloy, mould powder used in continues casting of steel and coke used in blast furnace.

For CMSX-4 alloy, the thermal diffusivity was found to increase with temperature below 1253 K with  $\gamma$  and  $\gamma'$  phases (NiTi and Ni Ti<sub>2</sub>) prevailing in the industrial samples. Between 1253 K and solidus temperature, these intermediate phases start dissolving in the matrix resulting in increased the structure disorder and consequent decrease the thermal diffusivity.

The experimental values of samples annealed at 1573 K and measured at 1277, 1403 and 1531 K did not show any noticeable change with time. These values were found to be lower than the thermal diffusivities of non-annealed samples. This observation is attributed to the completion of the dissolution of the  $\gamma$  and  $\gamma'$  phases in the matrix and the attainment of thermodynamic equilibrium.

Liquid CMSX-4 does not show any change of thermal diffusivity with temperature. It could be due to the decrease of the mean free path below characteristic distance between two neighbouring atoms.

The thermal diffusivities of mould powder having glassy and crystalline state decrease with an increasing temperature at lower temperature and are constant at higher temperature except for one glassy sample.

The thermal diffusivity measurements of mould powder in liquid state do not show any significant change with temperature. It is considered that this is likely to be due to the silicate network being largely broken.

The thermal diffusivity is increased with increasing crystallisation degree of mould powder.

Thermal diffusivity measurements of coke samples taken from taken from different level in the shaft of the blast furnace show that coke from deeper levels of the blast furnace exhibit larger thermal diffusivities. This is confirmed by XRD measurements showing increase of the value of larger average crystallite size along the structural  $c$ -axis,  $L_c$  (which is indicative of the degree of graphitisation) with depth in the blast furnace. The coke sample having higher degree of graphitisation shows larger thermal diffusivity. The XRD measurements of coke samples show that the graphitisation of coke was instantaneous between room temperature and 1473 K.

## **6. Future work**

1. Study the effect of deformation percentage on the thermal conductivity of austenitic stainless steel.
2. Thermal conductivity measurements of Ti, stainless steel alloys and plain carbon steel.
3. Further investigations of the thermal conductivity of blast furnace coke.

## References

- [1] Ormerod, R.Tylor, J.Edward, Metal Technology, April, 1978.p.p 109- 113.
- [2] KC. Mills, A.P. Day, P.N.Qusted, Estimation the Thermophysical Laboratory, Teddington, Middx.
- [3] A.V. Oelreich, M.Sc. Thesis, Royal Inst.of tech.,Div.Mat.Proc.Sci.,(2004), ISRN KTH/MSE--04/20--SE+ THMETU/EX.
- [4] M. Kawakami, T.Karato, H.Tagata, T.Takenaka, S.Yokoyama ,Science and Technology of Innovative Ironmaking for aiming at Energy Half Consumption, November 27 to 28, 2003, Tokyo, Japan, pp 49-53.
- [5] M. Hayashi<sup>1)</sup>, S. Gupta<sup>2)</sup>, T. Miyamoto<sup>3)</sup>, R. Abdul Abas<sup>1)</sup>, and S. Seetharaman<sup>1)</sup>, 'Thermal diffusivity of cokes taken from a pilot blast furnace', Department of Materials Science and Engineering, Royal Institute of Technology, Stockholm, Sweden unpublished research, (2003).
- [6] M.Hayashi, P.Fredriksson, S.Seetharaman, Science and Technology of Innovative Ironmaking for aiming at Energy Half Consumption, November 27 to 28, 2003, Tokyo, Japan, pp. 141-149.
- [7] H. Shibata, T. Emi, Y. Waseda, K. Kondo, H. Ohta and K. Nakajima: *Tetsu-to-Hagane*, 82, (1996), 504.
- [8] R. Taylor and K. C. Mills: *Ironmaking and Steelmaking*, 15 (1988), 187.
- [9] P.Qusted, National Physical Laboratory. Middx, UK, 2002.
- [10] P. Debye: Vorträge über die kinetische Theorie der Materie und Elektrizität, Gottinger Wolfskehlvortrage. B. G. Teubner, Leipzig and Berlin, (1914), 46.
- [11] G. Grimvall, "Thermophysical Properties of Materials", Publ. Elsevier Science B.V., Amsterdam, 1999.
- [12] A.Hazatte, B.Perrot, P.Archambault, Collque C7, supplement au Journal de Physique III,Volume 3, November 1993, p.p. 351-354.
- [13] H. Shibata, T. Emi, Y. Waseda, K. Kondo, H. Ohta and K. Nakajima: *Tetsu-to-Hagane*, 82 (1996), 504.
- [14] W. D. Kingery, H. K. Bowen and D. R. Uhlmann: Introduction to Ceramics, John Wiley & Sons, Inc., New York, (1976), 612.
- [15] B. O. Mysen, D. Virgo and C. M. Scarfe: *Am. Mineralogist*, 65 (1980), 690.
- [16] K. C. Mills: Slag Atlas, 2nd. ed., ed. by Verein Deutscher Eisenhüttenleute, Verlag Stahleisen GmbH, (1995), 6.
- [17] M. Hayashi, T. Watanabe, K. Nagata and S. Hayashi: Tokyo Institute of Technology, unpublished research, (2002).
- [18] M. Hayashi, N. Nabeshima, H. Fukuyama and K. Nagata: *ISIJ International* 42 (2002), 352.
- [19] R. Eriksson, M. Hayashi and S. Seetharaman: *Inter. J. Thermophys.*, 24 (2003), 785.
- [20] H.P.Klug, L.E.Alexander, X-ray diffraction procedures, John Wiley & Sons, Inc., USA, 2:nd Ed., (1974).pp. 700-702.
- [21] E. Fitzer, S. Weisenburger, Carbon, 1976,14, pp.323-327.